SUB-DAILY EARTH ROTATION DURING THE EPOCH '92 CAMPAIGN

A. P. Freedman, R. Ibañez-Meier, S. M. Lichten, J. O. Dickey

Jet Propulsion Laboratory, California Institute of Technology, Pasadena, California

T. A. Herring

Department of Earth, Atmospheric, and Planetary Sciences,

Massachusetts Institute of Technology, Cambridge, Massachusetts

Submitted to Geophysical *Research Letters*, November 1993

Abstract. Earth rotation measurements were obtained using Global Positioning System (GPS) data for 11 days during the Epoch '92 campaign in the Summer of 1992. Earth orientation was measured simultaneously with several very long baseline interferornetry (VLBI) networks. These data were processed to yield both GPS and VLBI estimates of UT1 with 3-hour time resolution, which were then compared and analyzed. The high frequency behavior of both data sets is similar, although drifts between the two series of ~0.1 ms over 2-5 days are evident, Models for tidally induced UT1 variations and estimates of atmospheric angular momentum (AAM) at 6-hour intervals were also compared with the geodetic data, These studies indicate that most of the geodetic signal in the diurnal and semidiurnal frequency bands can be attributed to tidal processes, and that UT1 variations over a few days are mostly atmospheric in origin.

Introduction

Variations in the rate of rotation of the solid Earth can result either from torques applied to the Earth from the exterior or interior or from mass redistributions within the Earth. For high-frequency Earth rotation variations, defined here as rotation rate changes occurring over time scales of one hour up to one week, the principal forces on the solid

Earth are thought to come from the atmosphere and oceans. Tidal forcing of the oceans is expected to dominate the rotational variations at periods of one day and less, while atmospheric winds should be significant at periods of a few days and longer.

High-precision techniques to monitor Earth rotation include very long baseline interferometry (VLBI), satellite laser ranging (SLR), lunar laser ranging (LLR), and, most recently, the Global Positioning System (GPS). VLBI estimates of Earth's rotation angle (UT1–UTC) at daily intervals and SLR estimates at roughly 3-day intervals have been made for several years, Over the past three years, measurements of UT] variations with hourly or so time resolution have been made sporadically by both VLBI and GPS [Herring and Dong, 1991; Lichten et al., 1992].

In association with the International GPS Geodynamics Service's (IGS) proof-of-concept campaign for the summer of 1992, an additional campaign known as SEARCH (Study of Earth-Atmosphere Rapid Changes) '92 was held to monitor high-frequency Earth orientation variations using all space geodetic techniques and to facilitate the collection of the best available related geophysical data [Dickey, 1993], Data were acquired from a variety of complementary techniques, especially during an intensive two-week period known as Epoch '92 (July 25-Aug. 8).

In this paper, we present GPS estimates of sub-daily variations in UT1 during Epoch '92 and compare them to those from VLBI, as well as to UT 1 variations expected from tide models and from atmospheric angular momentum computations. (In a companion study, we examine the accuracy of sub-daily estimates of polar motion [Ibañez-Meier et al., 1993, in preparation]). These intercomparisons should provide a robust estimate of Earth's true rotational variations during Epoch '92 over periods as short as a few hours, and help to improve our knowledge of the physical processes acting over these time scales.

Earth rotation time series

GPS

GPS data processing was performed with the JPL GIPSY/OASIS 11 software using strategies [Lichten, 1990, for example] that arc summarized in Table 1. Data from a network of 25 stations tracking a GPS constellation of 17 satellites were acquired over 11 days during the last week of July and first week of August, 1992. Due to the use of anti-spoofing (AS) signal encryption over the weekend (which the receiver software could not at that time handle properly), these data are not continuous but are divided into two groups from which multi-day GPS orbit arcs were created, Corrections to a nominal UT1 series (derived from the IERS Bulletin B [IERS, 1992]) were estimated from the data every 30 minutes. UT1 was modeled as a first-order autoregressive (AR 1) or Gauss-Markov process with a steady-state sigma of 0.06 ms and a time constant of 4 hours. Thus, over 30 minutes, 0.028 ms of process noise was added in quadrature,

We generated UT 1 time series using a variety of orbit modeling strategies [Freedman et al,, 1992; 1993], Our preferred strategy employed multi-day orbit arcs wherein one set of epoch satellite states (position and velocity) was estimated for each satellite. To allow for satellite force mode] deficiencies, three AR1 stochastic solar radiation parameters for each satellite were estimated hourly, Alternative estimation strategies yield UT 1 series that are somewhat different but which lead to similar conclusions,

For comparison with VLBI data, we constructed a smoothed GPS UT 1 data set, We began with the above 30-minute solution and applied a Gaussian filter with a half-width of about one-half hour to smooth and interpolate the GPS data to the epochs of the VLBI data. This time series contains GPS-derived UT1 measurements every 3 hours.

VLBI

VLBI data were acquired from the three networks described in Table 2. On certain days, UT1 was measured by more than one VLB1 network, enabling an assessment of the quality of the VLBI data. The correlated VLBI data were combined using the

NASA/GSFC, CfA/MIT-developed Kalman filter programs CALC and SOLVK [Herring et al., 1990; Ma et al., 1992]. UT], polar motion, nutation corrections, and station troposphere parameters were estimated over 24 hour time spans, with UT 1, polar motion, and the troposphere parameters modeled as random walks.

A number of solutions were generated in which UT 1 was estimated at intervals ranging from 30 minutes up to 6 hours. In the VLBI series shown below, UT 1 was estimated every 3 hours, with 0.04 ms of uncertainty added in quadrature after a diurnal and semidiurnal a priori tide model [Herring and Dong, 1993] had been applied. Since some days had more than one set of measurements and no one VLB1 network was run continuously over more than three days, a final smoothed VLBI solution was obtained by combining the 24-hour data sets from all the networks using a mild Gaussian filter with a full-width half-maximum of 3 hours.

Tide models

Two models for tidally-induced diurnal and semidiurnal UT] variations, one theoretical, one empirical, were compared with the GPS data, The theoretical model, referred to as the Gross [1993] tide model, is based on the oceanic angular momentum model of Seiler [1991], This formulation also contains corrections to the standard Yoder et al. [1981] tide model for non-equilibrium ocean tides at fortnightly and monthly periods. The empirical mode], referred to as the Herring tide model [Herring and Dong, 1993], is based on 8 years of VLBI UT 1 measurements. It includes estimates of the diurnal and semidiurnal tidal terms only. Note that this empirical time series may contain additional diurnal signal other than that due to the non-equilibrium ocean tides, due, for instance, to the atmosphere,

AAM

If angular momentum were exchanged solely between the atmosphere and the solid Earth, atmospheric angular momentum (AAM) variations would result in corresponding changes in the length of the day (LOD), the time derivative of UT1. Several sets of AAM

were computed every 6 hours as part of the SEARCH/IGS effort by three meteorological centers: the U. S. National Meteorological Center (NMC), the European Center for Medium-Range Weather Forecasts (ECMWF), and the Japanese Meteorological Agency (JMA). For each center, the AAM quantity that we use consists of the χ_3 AAM wind term integrated to the top of the model atmosphere (either 10 or 50 mbar, depending on center) plus the full (not inverted-barometer) pressure term [Barnes et al., 1983]. Gaps in the AAM series were filled by linear interpolation. A composite AAM series was then constructed by averaging the three AAM series together, thus reducing center-dependent errors.

We used this data set to estimate atmospherically induced variations in UT1. Since AAM mimics LOD, the AAM series must be integrated to be compared to a UT1 series. However, two arbitrary constants, equivalent to biases in LOD and UT1, enter into this integration. For the comparisons shown below," linear models were removed from the AAM and geodetic UT1 series to account for these constants.

Results

GPS vs. *VLBI*

The interpolated and smoothed time series of UT 1 at 3 hour intervals derived from both GPS and VLBI are shown in Figure 1. Typical forma] errors of the various data sets used in generating the smoothed UT 1 curves are summarized in Table 3, The UT1 values have been difference with the nominal Bulletin B smoothed reference series [IERS, 1992], thus removing both longer period UT1 variations and the Yoder et al. [1981] short-period tides from the displayed time series. The offset between the GPS and VLBI curves is arbitrary. Note the gap in GPS data due to AS during the weekend of August 1-2. The 6-day time span at the end of July where data exist from both techniques is referred to below as period A, while the 4.5-day time span in August is referred to as period B.

Although there appears to be a drift between the two series over several days, their diurnal variability is similar. If the two series are differenced, linear trends can be fit separately to periods A and B to quantify both the drift and residual scatter in GPS minus VLBI. These values are given in Table 3. Over 4 to 6 day time spans, GPS shows a drift with respect to VLBI of 20 to 40 μsec/day. After removing these drifts, the total RMS scatter is 0.023 ms,

The relationship between GPS and VLBI may be further explored by studying power spectra of the GPS and VLBI UT] and their difference (Fig. 2). Power spectra were obtained separately for the two periods A and B (after padding them with zeros to the same length) and averaged together. A 3-point spectral smoothing was used (corresponding to a bin width of 0.375 cycles per day), Both the VLB1 and GPS series show similar power in the diurnal and semidiurnal bands. Differencing the two time series removes the peaks in power at both frequencies, indicating that each series is measuring a true signal in these bands. This signal is primarily tidal in origin, as shown below.

GPS vs. *tide models*

In Figure 3 we compare GPS UT1 to the two models of tidally-induced UT1 variations. The GPS series for each period (A and B) has had a best-fitting quadratic subtracted to remove longer-period fluctuations. Note that the empirical Herring model more accurately reflects the observed UT 1 variations than does the theoretical Gross model,

Power spectra of the GPS UT1 series and the GPS series difference with each tide model are shown in Fig, 4. The Herring model removes most of the excess power in the diurnal and semidiurnal bands, with a hint of signal remaining at 2 cycles per day (cpd). The Gross model removes some power at diurnal frequencies, but adds substantial power at semidiurnal frequencies (as seen in Fig. 3). These differences are quantified in Table 3, which shows the RMS scatter of the three time series whose spectra are plotted in Fig. 4. The empirical model is more consistent with the observed UT 1 than is the theoretical

model at both diurnal and semidiurnal frequencies. This may be due to deficiencies in the theoretical ocean model or to additional non-oceanic signal at these frequencies.

GPS *vs. AAM*

The average AAM time series numerically integrated to generate "atmospheric" UT] is shown in Figure 5. Also shown are the UT1 variations expected from the longer-period. (14 and 30-day) non-equilibrium ocean tides emerging from the numerical ocean model [Gross, 1993], and a GPS UT1 series incorporating the Bulletin B reference series to restore its multi-day variability, Each time series for each of periods A and B has had a best-fitting bias and trend removed. The AAM can account for the overall shape of the GPS UT 1 curve, and the longer-period tide corrections do not add substantial power at these few-day periods. Although the original AAM series exhibits a marked diurnal signature, when integrated to form UT1, the daily variability is negligible.

The sum total of the integrated AAM, diurnal and semidiurnal tides (from Herring), and longer-period tides (from Gross) is shown in Figure 6a, together with the observed UT1 variations from GPS and VLBI. Linear trends were removed from each series for each period, Most of the geodetic signal can be described as the sum of AAM variations and tidally induced UT1, with the tides acting at periods of one day and less and AAM acting at periods greater than a day. The residual signal in the geodetic data not accounted for by the AAM or the tide models is shown in Fig, 6b, and the RMS scatter of this difference is given in Table 3 for all three AAM data sets as well as the average AAM series, The differences between GPS and VLBI are comparable in size to those between the AAM and geodetic series. No center or technique stands out as superior, and all differences are consistent with the typical GPS and VLBI formal errors of about 0.02 ms.

Conclusions

Differences between the various series considered here tend to be at the level of 0.02 to 0,03 ms, consistent with the formal uncertainties of the data themselves. The main exception is the theoretical tide model, which simply does not agree with the geodetic

data, There is also a drift in the GPS data relative to VLBI which, over time spans of 6 days or so, appears to be linear. This drift is probably due to systematic effects such as orbit mismodeling in the GPS estimation process, and it must be removed before using GPS estimates over time scales of more than a few days.

Both GPS and VLBI UT1 estimates exhibit nearly identical variability in the diurnal and semidiurnal bands, in agreement with a model for tidal variations whose values were derived from many years of geodetic VLBI data. There is no residual tidal signal that exceeds the error level estimated for the data, although additional signals with amplitudes smaller than 0.02 ms could certainly be present. Although the theoretical tide model does not agree with observations in either band, the disagreement is largest in the semidiurnal frequency band.

The AAM-derived UT1 curve exhibits variability consistent with that of geodetic UT1 at periods longer than one day. The sub-daily variability due to AAM is quite small, however, and cannot be disentangled from oceanic tidal effects and noise in the geodetic data. However, limits can be placed on the size of any residual AAM signal.

The GPS UT 1 time series can thus be represented by the sum of four effects: ocean tides at diurnal and semi-diurnal periods, AAM fluctuations at periods longer than one day, a linear drift in UT1 due possibly to orbit mismodeling, and a broadband noise component. To accurately estimate UT] at these frequencies, the tidal variations in UT1 must certainly be considered, either by explicit use of the Herring tide model or by allowing adequate variability in UT1. Further research is necessary to investigate and reduce both the drift in UT1 of -0.1 rns over 2-5 days, and the level of noise present in the data.

Acknowledgments. The authors thank the many people involved in collecting and processing the vast quantities of data from both GPS and VLBI, as well as the people and institutions involved in generating the AAM data sets. The work of APF, RIM, SML, and JOD described in this paper was carried out by the Jet Propulsion Laboratory, California Institute of Technology, under contract with the National Aeronautics and Space

Administration (NASA), The work of TAH was supported by the National Science Foundation under grant EAR-89-05560, by NASA under grant NAG 5-538 and NAW-0037, by the National Oceanic and Atmospheric Administration (NOAA) under grant NA90AA-D-AC481, and by the Kerr-McGee Foundation. The views expressed herein are those of the authors and do not necessarily reflect the views of NOAA or any of its subagencies.

References

Barnes, R. T. H., R. Hide, A. A. White, and C. A. Wilson, "Atmospheric Angular Momentum Fluctuations, Length-of-Day Changes and Polar Motion," *Proc. R, Sot. London, Ser.* A, 387,31-73, 1983.

Dickey, J. O., "High Time Resolution Measurements of Earth Rotation," in *Advances in Space Research,* Pergamon, in press, 1993.

Freedman, A. P., R. Ibañez-Meier, J. O. Dickey, S. M. Lichten, and T. A. Herring, "Sub-Daily Earth Rotation Determined With GPS: Recent Results (abstract)," *EOS, Trans. A.G. [J.,* 73 (43), Fall Meeting Suppl., 135, 1992,

Freedman, A. P., R. Ibañez-Meier, J, O. Dickey, S. M. Lichten, and T. A. Herring, "GPS Measurements of Sub-Daily Earth Rotation During the Epoch '92 Campaign," *TDA Progress Report,* in preparation, Jet Propulsion Laboratory, Pasadena, California, 1993.

Gross, R. S., "The Effect of Ocean Tides on the Earth's Rotation as Predicted by the Results of an Ocean Tide Model," *Geophys.* Res. *Lett.,* 20,293-296, 1993.

Herring, 'I'. A., J. L. Davis, and 1. I. Shapiro, "Geodesy by Radio Astronomy: The Application of Kalman Filtering to Very Long Baseline lnterferometry," *J. Geophys. Res.,* 9S, 12561-12581, 1990,

Herring, T. A., and D. Dong, "Current and Future Accuracy of Earth Rotation Measurements," in *Proceedings of the AGU Chapman Conference on Geodetic VLBI:*

Monitoring Global Change, pp. 306-324, NOAA Tech. Rep, NOS 137 NGS 49, NOS/NOAA, Rockville, MD, 1991.

Herring, T. A., and D. Dong, "Measurement of Diurnal and Semidiurnal Rotation Variations and Tidal Parameters of the Earth," *J. Geophys. Res.,* submitted, 1993.

Ibañez-Meier, R., A. Freedman, R. Gross, U. Lindqwister, and S. Lichten, "Subdaily Polar Motion Measurements With the Global Positioning System," *Geophys. Res, Lett.,* in preparation, 1993,

IERS, *1991 IERS Annual Report,* International Earth Rotation Service, Central Bureau of the IERS–Observatoire de Paris, July, 1992.

Lichten, S. M., "Estimation and Filtering for High-Precision GPS Positioning Applications," *Man. Geod., 15, 159-176, 1990.*

Lichten, S. M., S. L. Marcus, and J. O. Dickey, "Sub-Daily Resolution of Earth Rotation Variations With Global Positioning System Measurements," *Geophys. Res. Lett.,* **19,** 537-540, 1992.

Ma, C., J. W. Ryan, and D. S, Caprette, "Crustal Dynamics Project Data Analysis-1991 VLBI Geodetic Results," in *NASA Tech. Memo 104552,* pp. NASA - Goddard Space Flight Center, Greenbelt, MD, 1992,

Seiler, U., "Periodic Changes of the Angular Momentum Budget Due to the Tides of the World Ocean," *J. Geophys. Res.,* 96, 10,287-10,300, 1991.

Yoder, C. F., J. G. Williams, and M. E. Parke, "Tidal Variations of Earth Rotation," *J. Geophys. Res.,* 86,881-891, 1981,

Table 1. GPS Estimation Strategy

Estimated parameters	
Station locations (8 fiducial sites)	Wet zenith troposphere (random walk)
Satellite states	Clock biases (white-noise)
Solar radiation pressure	Carrier phase biases
UT1 (AR1)	Polar motion (white noise)
Standard models	
Solid Earth tides and equilibrium ocean tides [198 1]	
Gravity field coefficients: GEMT3, 8x8 truncation	
Nutation mode]: 1980 IAU model	
A priori and fiducial site locationsITRF91	
Nominal UTPM from IERS Bulletin B	
Rogue receivers: Pseudorange (1 m), Carrier Phase (1 cm)	
6-minute data interval (obtained by decimation)	

Table 2. VLBI Data

NASA's Goddard Space Flight Center (GSFC) - "NASA R&D"	
8 experiments; 5-6 sites in N. America, Hawaii, and Europe	
NOAA's Laboratory for Geosciences - "IRIS"	
4 experiments (one mobile, three IRISA); 5 sites in N. America and Europe	
Unites States Naval Observatory (USNO) - "NAVNET"	
6 experiments; 4-6 sites, located around globe	

Notes: Data were obtained from July 26 through August 11.
Four days have measurements by both NAVNET and NASA R&D.
Formal errors differ significantly from experiment to experiment,

Table 3. Statistics

Typical 30-Minute UT] Formal Errors

GPS	IRIS	NAVNET	NASA R&D
0,02-0.03 ms	*0.02-0.04* 111s	0.01 S-0.04 ms	0.01-0.025 ms

GPS Minus VLBI

	Period A	Period B	Entire time span
slope	-0.018 ms/day	0.041 ms/day	- .
RMS scatter	0.022 ms	0.026 ms	0.023 ms

GPS Minus Tides

	GPS UT1 only	GPS minus Herring	GPS minus Gross
RMS Scatter	0,032 ms	0.018 ms	0,035 ms

UT1 Minus (AAM+Tides)

RMS Of difference	Average AAM	NMC AAM	ECMWF AAM	JMA AAM
GPS UT1	0.020 ms	0.021 ms	0.022 ms	0.019 ms
VLBI UT1	*0.023* ms	*0.027* ms	*0.022* ms	*0.022* ms

Figure Captions

Fig. 1. UT] from GPS and VLBI evaluated every 3 hours.

Fig. 2. Power spectra of the GPS, VLBI, and GPS–VLBI UT1 series,

Fig. 3. GPS UT] and two models of tidally induced UT1 variations.

Fig. 4. Power spectra of the GPS UT1 series and the GPS series difference with each of the two tide models.

Fig. 5. Comparison of integrated average AAM and longer-period tides with geodetic UT] .

Fig. 6. a) Sum of the integrated AAM, diurnal and semidiurnal tides, and longer-period tides, compared to the observed UT1 variations from GPS and VLBI; b) Geodetic UT1 with the tidal terms and AAM contributions removed. A typical GPS/VLBI formal error is illustrated.

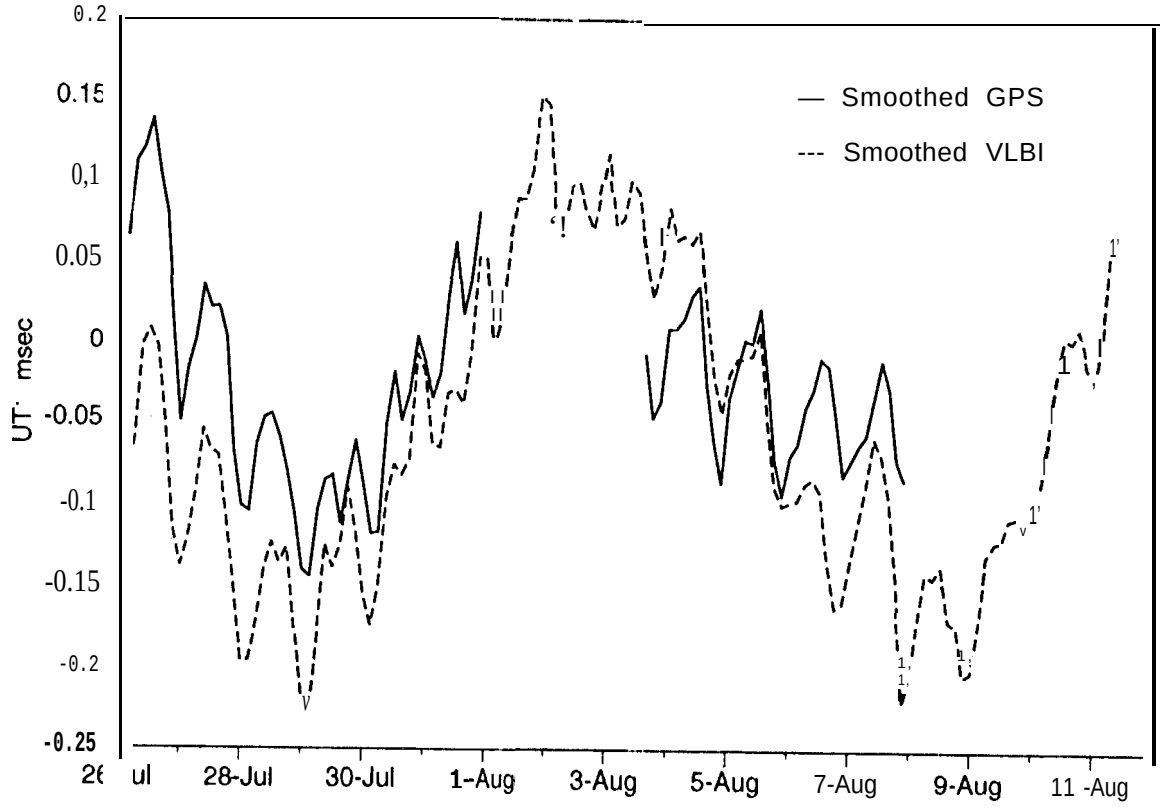
0.2
0.15
0,1
0.05
0
-0.05
-0.1
-0.15
-0.2
-0.25
UT· msec
— Smoothed GPS
--- Smoothed VLBI
28-Jul
30-Jul
1-Aug
3-Aug
5-Aug
7-Aug
9-Aug
11 -Aug

Fig. 1

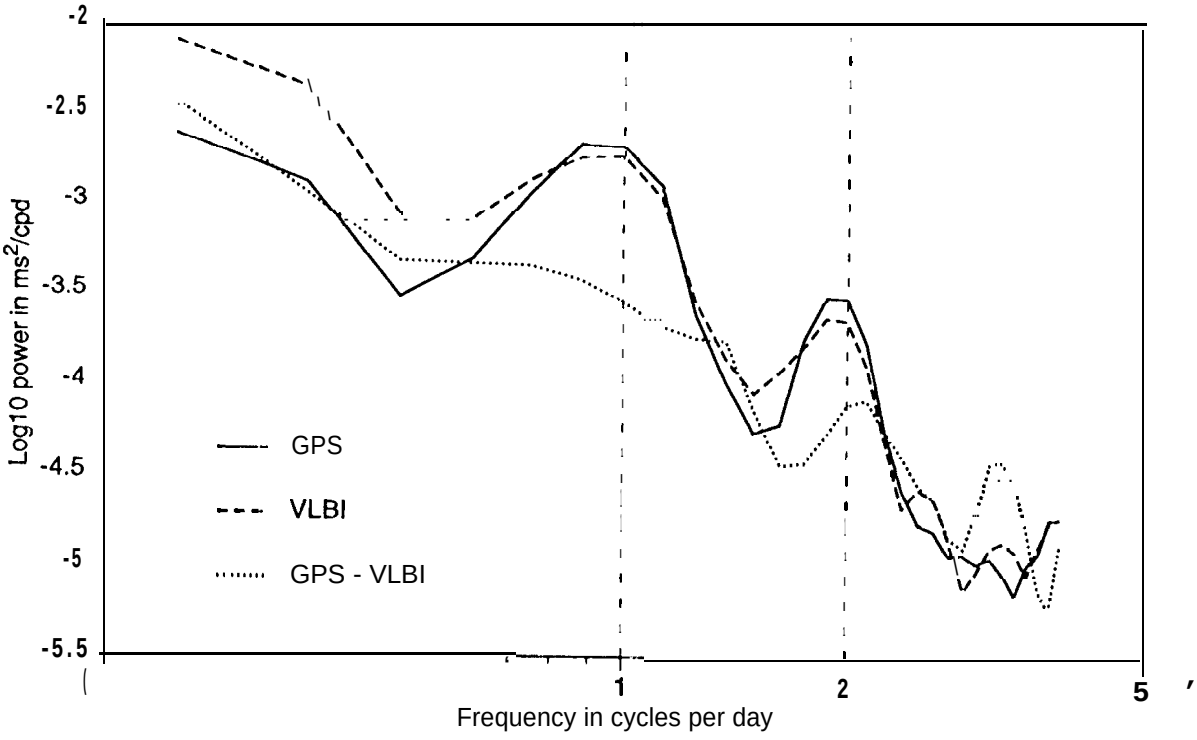
-2
-2.5
-3
-3.5
-4
-4.5
-5
-5.5
Log10 power in ms²/cpd
GPS
VLBI
GPS - VLBI
1
2
5
Frequency in cycles per day

Fig. 2

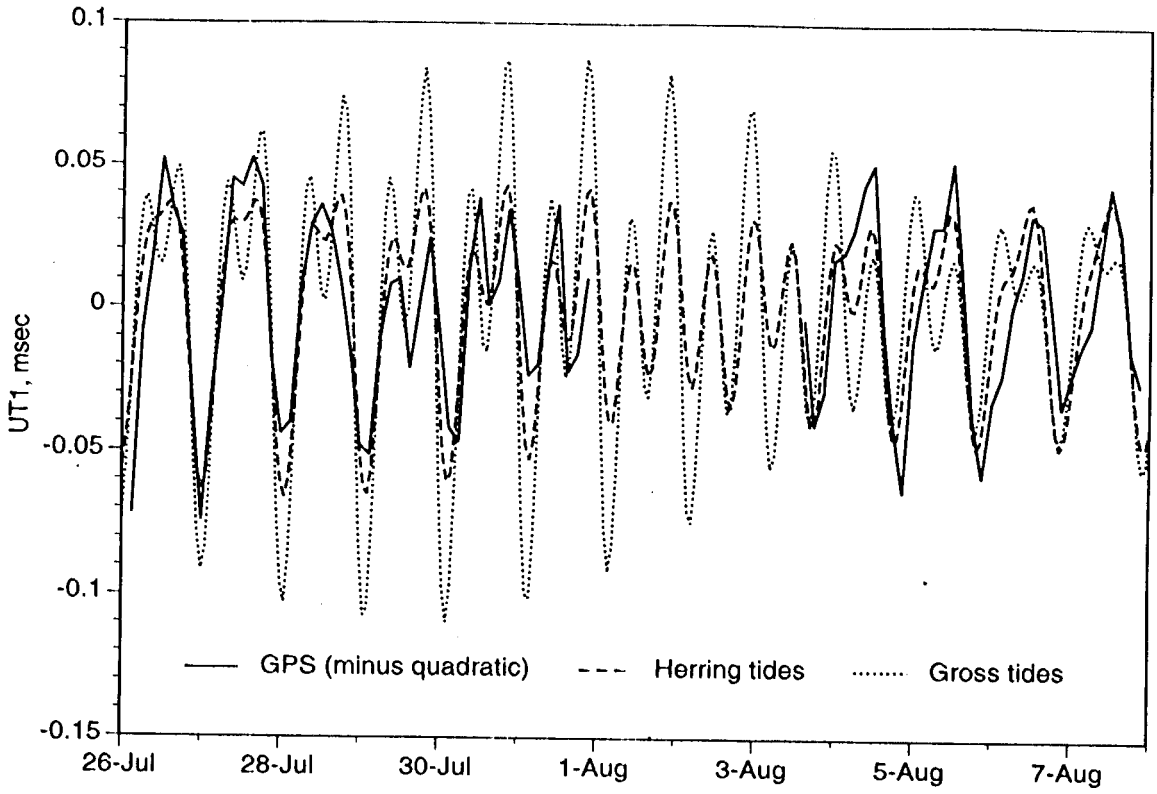
0.1
0.05
0
-0.05
-0.1
-0.15
UT1, msec
GPS (minus quadratic)
Herring tides
Gross tides
26-Jul
28-Jul
30-Jul
1-Aug
3-Aug
5-Aug
7-Aug

Fig. 3

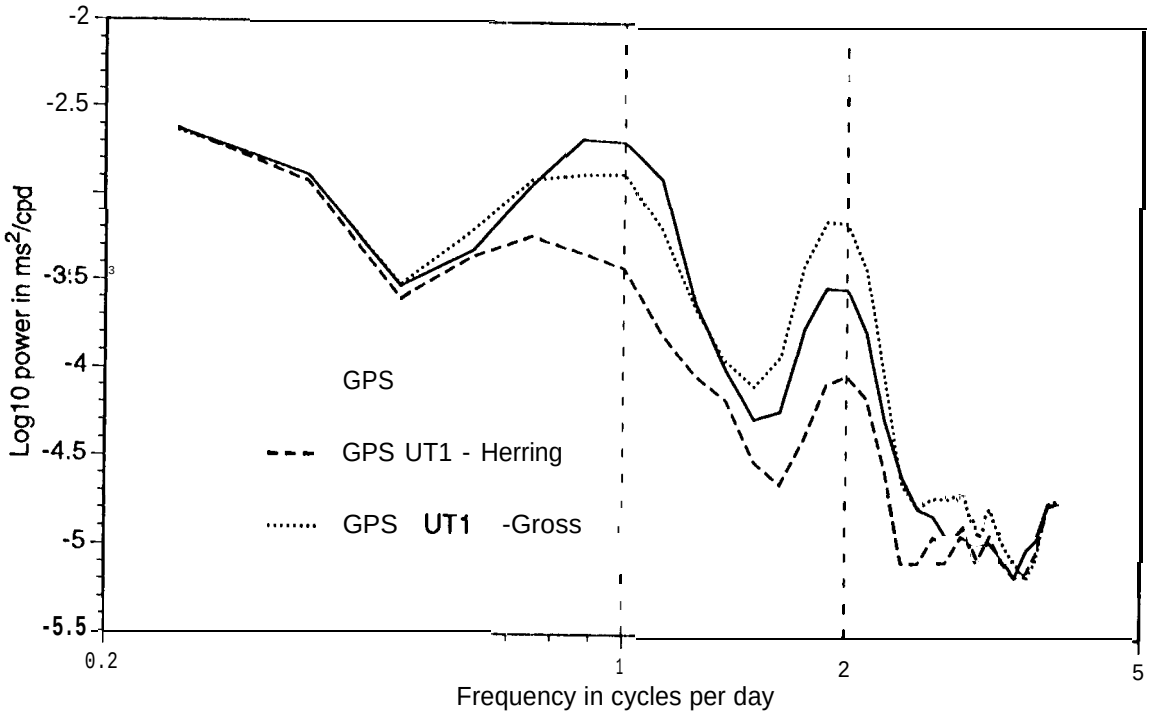
-2
-2.5
-3
-3.5
-4
-4.5
-5
-5.5
Log10 power in ms2/cpd
GPS
GPS UT1 - Herring
GPS UT1 -Gross
0.2
1
2
5
Frequency in cycles per day

Fig. 4

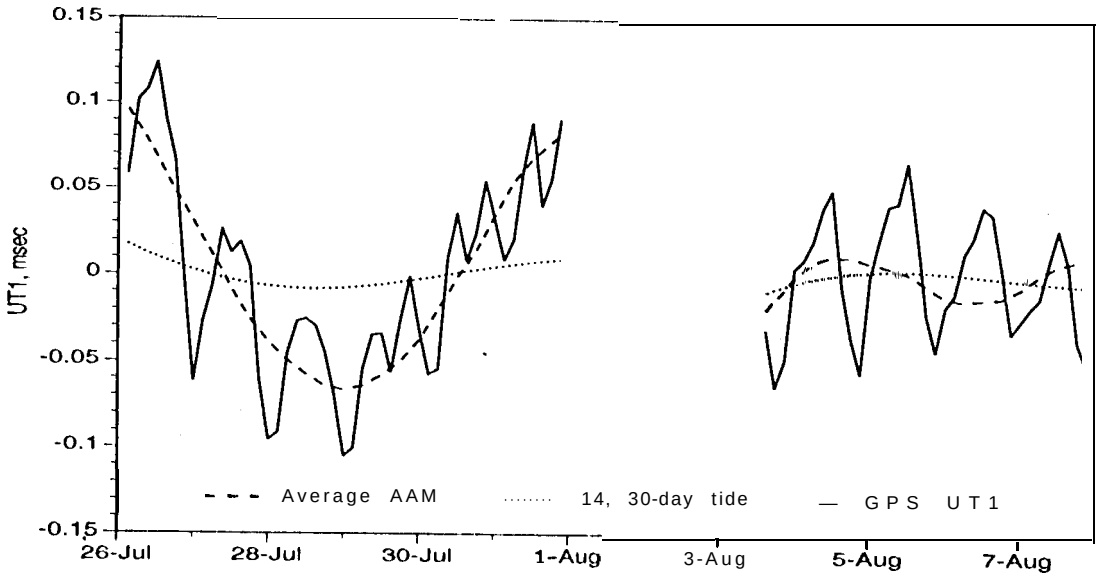

Fig. 5

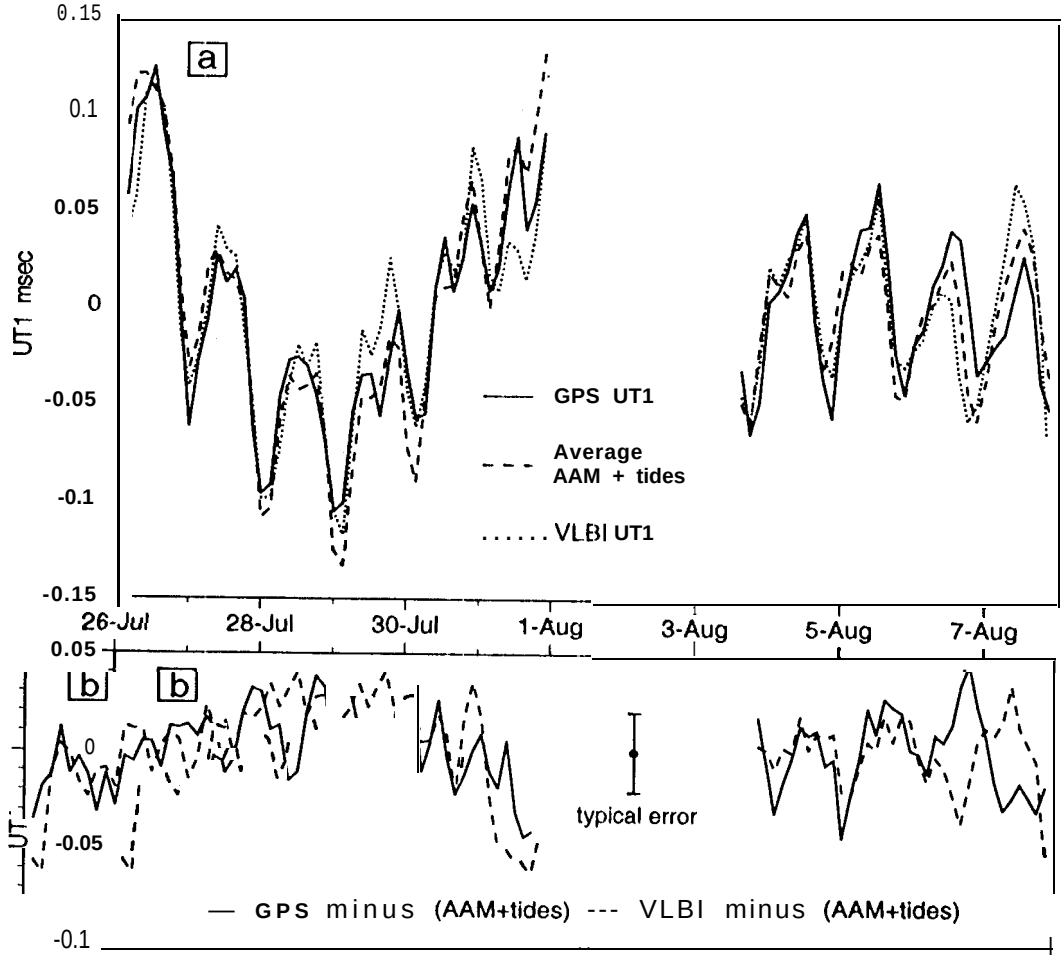

Fig. 6a) (upper) and b) (lower)